Self-Organization and Polyolefin Nucleation Efficacy of 1,3:2,4-Di-*p*-Methylbenzylidene Sorbitol

THOMAS A. SHEPARD,[1,*] CARL R. DELSORBO,[†] RICHARD M. LOUTH,[‡] JONATHAN L. WALBORN,[¶] DAVID A. NORMAN,[§] NOEL G. HARVEY,[2] RICHARD J. SPONTAK[1]

[1] Department of Materials Science & Engineering, North Carolina State University, Raleigh, North Carolina 27695-7907

[2] Polymer Science & Technology Department, Becton Dickinson Research Center, Research Triangle Park, North Carolina 27709-2016

Received 15 October 1996; revised 9 June 1997; accepted 16 June 1997

ABSTRACT: Recent studies have demonstrated that addition of a small quantity of dibenzylidene sorbitol (DBS) to a molten polymer may result in a physical gel if conditions permit the DBS molecules to self-organize into a three-dimensional network composed of highly connected nanofibrils. If the polymer crystallizes, DBS may also serve as a nucleating agent, promoting the formation of spherulites, especially in commercially important polyolefins such as polypropylene. We examine the thermal and mechanical properties, as well as the morphological characteristics, of an isotactic polypropylene copolymer with 3 wt % ethylene upon addition of less than 1 wt % of 1,3:2,4-di-*p*-methylbenzylidene sorbitol (MDBS). From dynamic rheological measurements, pronounced complex viscosity increases, attributed to MDBS nanofibril network formation, are observed at concentration-dependent temperatures above the melting point of the nucleated copolymer. Transmission electron micrographs of RuO_4-stained sections confirm the existence of MDBS nanofibrils measuring on the order of 10 nm in diameter and, at higher concentrations, fibrillar bundles measuring up to about 200 nm across and several microns in length. The addition of MDBS at different concentrations is also found to promote increases in optical clarity, yield strength, tensile strength, and ultimate elongation of modified copolymer formulations. © 1997 John Wiley & Sons, Inc. J Polym Sci B: Polym Phys **35:** 2617–2628, 1997

Keywords: dibenzylidene sorbitol; polymer crystal nucleation; polypropylene; clarifying agent

INTRODUCTION

Dibenzylidene sorbitol (DBS) is a low-molar-mass organic molecule that is capable of physically gelling organic liquids and polymeric melts. The chemical structure of this butterfly-shaped amphiphile, also referred to as 1,3:2,4-dibenzylidene sorbitol, is shown in Figure 1. Due to the presence of two hydroxyl groups, DBS molecules can strongly interact through hydrogen bonding and, under suitable conditions, self-organize into a three-dimensional nanofibrillar network. Recent experimental efforts have shown that DBS induces thermoreversible gelation in numerous common solvents such as *o*/*p*-xylene, 1,4-dioxane, benzene, acetonitrile, and ethylene glycol.[1–6] According to the results of Yamasaki and Tsutsumi,[4] both the critical gel concentration and the morphology of the resultant DBS network depend

* *Present address:* Polymer Science & Technology, Becton Dickinson Research Center, Research Triangle Park, NC 27709

† *Present address:* Department of Materials Science & Engineering, University of Alabama, Birmingham, AL 35294

‡ *Present address:* Industrial Manufacturing, Albany, GA 31707

¶ *Present address:* IVAC Medical Systems, Creedmoor, NC 27522

§ *Present address:* Department of Materials Science & Engineering, University of Michigan, Ann Arbor, MI 48109

Correspondence to: R. J. Spontak

Journal of Polymer Science: Part B: Polymer Physics, Vol. 35, 2617–2628 (1997)
 CCC 0887-6266/97/162617-12

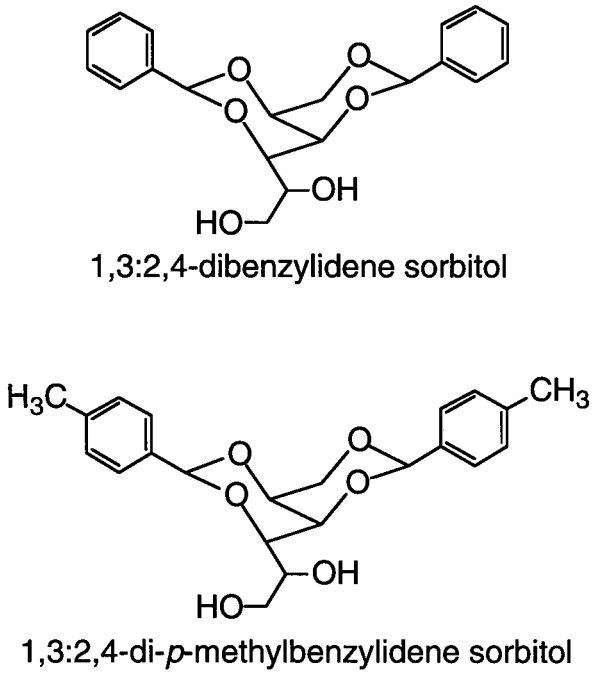

Figure 1. Chemical structures of 1,3:2,4-dibenzylidene sorbitol (DBS, top), and 1,3:2,4-di-*p*-methylbenzylidene sorbitol (MDBS, bottom). Note that these molecules appear to be butterfly-shaped, which may help to promote their ability to self-assemble in various liquid environments.

strongly on solvent polarity, as expressed in terms of the proton donor number. Physical gels likewise are produced at ambient temperature when a small quantity (typically < 3 wt %) of DBS is added to polydimethylsiloxane,[7–9] polyalkylene oxides (e.g., polypropylene glycol),[10,11] and poly(dimethylsiloxane-*g*-alkylene oxide) graft copolymers.[7,10,12]

If a DBS-modified molten polymer such as polystyrene or polycarbonate undergoes vitrification as it cools from the melt to ambient temperature, the DBS molecules phase-separate into aggregates that, according to light scattering,[13] measure on the order of 100–200 nm in size. In the presence of crystallizable polymer chains, DBS induces gelation[14,15] at temperatures above the polymer melting temperature (T_m) and subsequently promotes heterogeneous crystal nucleation at reduced temperatures.[6,16–23] As a nucleating agent, the high-surface-area DBS nanofibrils (at $\approx$ 400 m^2/g, assuming nanofibrils 10 nm in diameter[6]) assist polymer chains to crystallize into numerous small spherulites, which, in turn, endow the polymer with enhanced mechanical strength and, depending on spherulite size, optical clarity. Thierry et al.[6] have proposed an efficiency scale based on seeded versus unseeded crystallization temperatures for nucleating agents used in conjunction with isotactic polypropylene. According to their scale, DBS is rated relatively highly at 41% (near 4-pyridinecarboxylic acid at 39%). To put this ranking in perspective, 4-biphenyl carboxylic acid is rated the highest at 66%, whereas 2,3-pyridine dicarboxylic acid is rated the lowest at 13%.

We examine the mechanical and thermal properties, as well as the morphological characteristics, of a polypropylene copolymer modified through addition of a chemical derivative of DBS, namely, 1,3:2,4-di-*p*-methylbenzylidene sorbitol (MDBS), which is illustrated in Figure 1. Note that MDBS can be described as DBS with two additional methyl groups, one on each of the terminal phenyl rings at the para position.

EXPERIMENTAL

Materials Preparation

The materials examined here were formulated from a stabilizer-free copolymer of 3% random ethylene in isotactic propylene. According to gel permeation chromatography, the $\bar{M}_n$ and $\bar{M}_w$ of this copolymer (designated iPPe) were 50,700 and 198,300 g/mol, respectively, prior to compounding. Five formulations were compounded under identical conditions from the copolymer and MDBS, obtained at 98% purity from Milliken Chemicals (Spartanburg, SC), at loadings of 0.0, 0.09, 0.18, 0.50, and 0.75 wt % MDBS by the Exxon Chemical Co. (Baytown, TX). Compounding was performed on each formulation, as well as on the non-nucleated iPPe control (0.0 wt % MDBS), in a 2.54 cm Killion compounder operated at 85 rpm with a high-work mixing screw. The feed throat and section/die temperatures were maintained at 180° and 215–220°C, respectively. (These temperatures were just below the melting temperature range of pure MDBS, 225–235°C. It should be noted, however, that complete dissolution of DBS and MDBS in liquids such as *o*-xylene and polydimethylsiloxane has been observed[7,9,12] at temperatures in the vicinity of 190°C.) Step plaques measuring 5.1 $\times$ 7.6 cm with thicknesses of 1.0 and 2.0 mm, as well as ASTM Type V tensile bars, were injection-molded from each formulation (including the control) in a 91-ton Arburg All-Rounder under identical thermal conditions (210°C nozzle temperature, 210–212°C zone 1–3 temperatures, and 25°C mold temperature) and pressures. Great care was exercised to guarantee

that the four nucleated formulations and the nonnucleated control possessed nearly identical thermal histories so that the concentration-dependent nucleation attributes of MDBS in the iPPe copolymer could be unambiguously identified.

Characterization Methods

Dynamic Rheology

A Rheometrics RMS800 mechanical spectrometer was employed to measure the temperature dependence of the complex viscosity of each iPPe formulation in the range 100–240°C. Disk-shaped specimens measuring 25 mm in diameter and 2 mm thick were cut from the injection-molded plaques so that tests could be conducted with 25 mm parallel plates separated by a 2 mm gap. Each specimen was initially heated to 242°C and held at that temperature for 4 min to insure complete melting of both the polypropylene and MDBS. The temperature was subsequently decreased in 2°C increments. At each step, the temperature was held constant for 1 min to promote quiescent specimen equilibration, and then a 2% strain was imposed at an oscillatory frequency of 10 rad/s. Testing was halted upon incipient iPPe solidification.

Transmission Electron Microscopy (TEM)

Each plaque was sectioned normal to the plaque surface with a 35° cryodiamond knife in a Reichert-Jung Ultracut-S ultramicrotome maintained at −100°C. Resulting sections obtained from the interior of each plaque (to avoid complications due to the presence of a surface) were collected on copper TEM grids and subsequently exposed to the vapor of 2% RuO_4(aq) for 5 min to stain the phenyl rings of the MDBS molecules. Electron micrographs were acquired on a Zeiss EM902 electron spectroscopic microscope operated at 80 kV and an energy loss (ΔE) of 0 eV.

Differential Scanning Calorimetry (DSC)

Melting temperatures were measured by differential scanning calorimetry on a Perkin-Elmer DSC4. A small piece of each specimen was sealed in an aluminum pan and heated from ambient temperature to 200°C at 10°C/min. It was then rapidly cooled at the maximum permissible, but unmeasurable, rate to ambient temperature so that a second analysis could be performed. Since the raw DSC data resembled classic thermograms of PP with little variation, they are not included here. (Examples of thermograms from MDBS-nucleated PP copolymers are provided in ref. 17.) Melting temperatures reported in this work correspond to the onset of the melting endotherm.

UV-Vis Spectrophotometry

The optical properties of each iPPe/MDBS formulation were analyzed at ambient temperature using a Shimadzu UV-2101 PC UV-Vis Scanning Spectrophotometer operated in the wavelength (λ) range from 400 to 700 nm. Absorption tests relative to the unmodified iPPe copolymer were conducted on the thin section (1.0 mm) of the step plaques described earlier. At least six scans were collected from each specimen to guarantee both reproducibility and specimen homogeneity.

Uniaxial Tensile Testing

The dogbone-shaped tensile bars produced during injection molding were subjected to uniaxial tensile deformation at ambient temperature on an Instron instrument. Most of the tensile data were obtained at a crosshead speed of 2.5 mm/min, but some experiments were conduced at 25 mm/min for comparison. The mechanical properties reported herein employ engineering (not real) stress.

RESULTS AND DISCUSSION

Evidence of MDBS Self-Organization

Figure 2 shows the variation of the complex viscosity (η^*) with temperature for molten iPPe specimens varying in MDBS concentration and cooled from 242°C. In the case of the neat iPPe copolymer (curve a in Fig. 2), η^* is seen to increase gradually and monotonically with decreasing temperature down to about 118°C, at which point it increases abruptly. This sudden and dramatic increase in η^* signifies the onset of iPPe solidification, and the temperature at which this transition occurs identifies the crystallization temperature (T_c) of the iPPe copolymer. Similar increases in η^* are likewise evident in the four remaining curves (b–d), which correspond to the iPPe copolymer with different concentrations of MDBS. Note that the temperatures at which this transition occurs are increased beyond that of the neat copolymer by more than 12°C (to between 130 and 135°C), thereby confirming the expectation that MDBS promotes iPPe crystallization through heterogeneous nucleation at temperatures higher than the

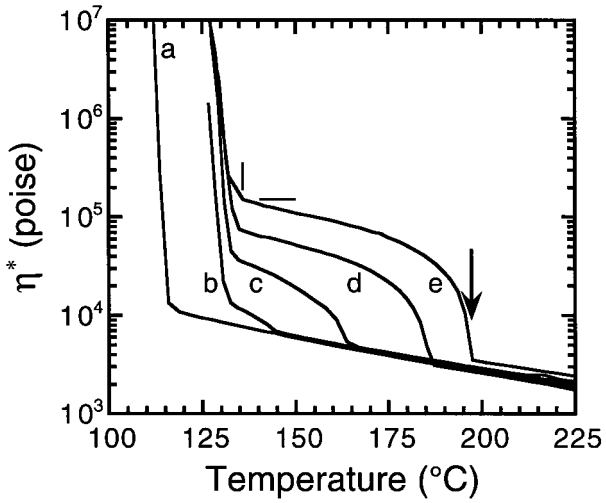

Figure 2. Complex viscosity (η^*) shown as a function of temperature upon cooling for the iPPe copolymer at five different concentrations of MDBS (in wt %): (a) 0.00, (b) 0.09, (c) 0.18, (d) 0.50, and (e) 0.75. The vertical and horizontal lines show the temperature and viscosity, respectively, at which the 0.75 wt % MDBS formulation crystallizes, while the arrow denotes the temperature at which MDBS-induced physical gelation commences in the same formulation.

T_c of the unmodified iPPe copolymer. Sterzynski et al.[17] report a comparable increase in T_c ($\approx$ 13°C) upon adding ca. 0.25 wt % MDBS to a random iPPe copolymer with similar ethylene content.

Crystallization temperatures are presented as a function of the weight percentage of MDBS (w_{MDBS}) in Figure 3 and indicate that T_c is virtually independent of w_{MDBS} when $w_{\mathrm{MDBS}} > 0.18$ in the present series. As seen in Figure 4, the melting temperatures (T_m) obtained from DSC are comparable in magnitude to the T_c measured by rheology for the formulations containing MDBS, indicating that the crystal morphology and population of the injection-molded specimens differ (due most likely to built-in stresses) from those of the specimens recrystallized in the rheometer. (In a separate study of MDBS-induced iPPe nucleation,[17] ΔT ($=T_m - T_c$) was found to decrease from about 47 to 32°C upon adding ca. 0.25 wt % MDBS.) The first DSC analysis ("heat") showed no discernible dependence of T_m on MDBS concentration. The subsequent analysis ("second heat") of the same specimens reveals, however, that the T_m from each formulation containing MDBS is measurably higher (beyond experimental uncertainty) than that of the neat iPPe copolymer. Also evident (Figure 4) is that T_m from the second heat, in the same manner as T_c (Fig. 3), becomes independent of w_{MDBS} as w_{MDBS} is increased. The T_c and T_m data reported above suggest that the nucleation efficacy of MDBS in iPPe reaches a saturation level at low w_{MDBS}. This apparent trend is consistent with limited x-ray diffraction data acquired[24] from the monoclinic α phase of the iPPe copolymers (not shown). Upon deconvolution analysis, these data imply that the degree of crystallinity increases from 66% for the unmodified iPPe copolymer to about 74% for all remaining MDBS formulations, yielding an overall increase in crystallinity of about 12%. According to Sterzynski et al.,[17] a 10.5% increase in crystallinity is achieved when a small quantity of MDBS is added to an iPPe copolymer.

Another interesting feature of Figure 2 is the presence of a plateau region, as well as a second thermal transition, at temperatures above T_c in each formulation. These transition temperatures, more clearly shown as a function of w_{MDBS} in Figure 3, are attributed to the onset of the sol $\rightarrow$ gel transition,[14,15] at which MDBS molecules self-organize into a three-dimensional nanofibrillar network in these iPPe melts. Note that, unlike the $T_c(w_{\mathrm{MDBS}})$ in Figure 3, the gelation temperature increases monotonically with increasing w_{MDBS} over the course of the w_{MDBS} examined in this work. In addition, the magnitude of the increase in η^* associated with the MDBS-induced gel state is also seen to increase with increasing w_{MDBS} in Figure 2. To illustrate this point more clearly, η^* is presented as a function of w_{MDBS} for four different isotherms in Figure 5. At low temperatures (e.g., 140°C, which is just above the T_c values shown in Figure 3), the difference in η^* of the 0.75 wt % MDBS formulation as compared to that of the neat iPPe melt is substantial (larger by a factor of $\approx 25\times$). As the temperature is increased, though, this variation in η^* becomes gradually less marked, until η^* becomes nearly independent of w_{MDBS} (and no gelation transition occurs) at 200°C.

From previous morphological studies of DBS in organic liquids[2,4–6] and polymer melts[7–9,12] at ambient and elevated temperatures, it is reasonable to expect that the self-organization of MDBS into a nanofibrillar network is responsible for the gelation transitions, as well as the accompanying viscosity increases, evident in Figure 2 and correlated with w_{MDBS} in Figures 3 and 5, respectively. Figure 6 displays a series of electron micrographs obtained from the five iPPe formulations under investigation here. Recall from the Experimental section that the MDBS molecules are preferentially stained with electron-dense RuO_4 and should

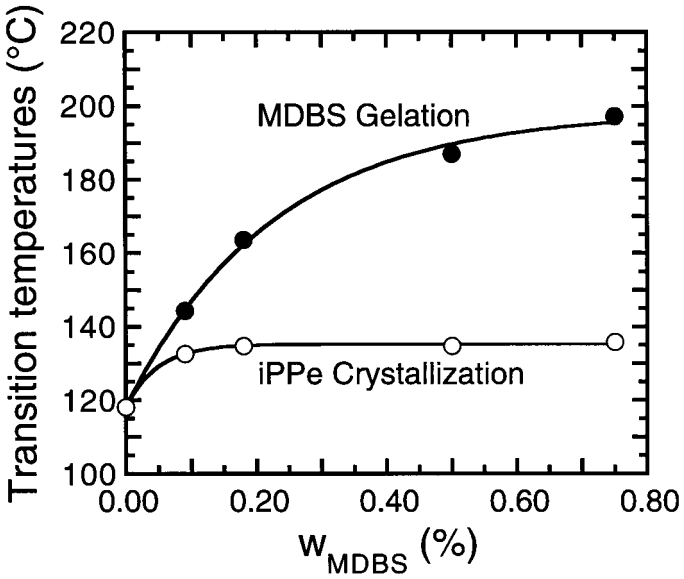

Figure 3. Phase-transition temperatures determined from the data in Fig. 2 and presented in terms of MDBS concentration (w_{MDBS}). The iPPe crystallization temperature (○) reaches a plateau and becomes independent of w_{MDBS}, whereas the MDBS-induced gelation temperature (●) increases monotonically over the range of w_{MDBS} examined. The solid lines are guides for the eye.

therefore appear dark in transmission. The absence of any stained microstructure in Figure 6a is consistent not only with the fact that this specimen corresponds to the unmodified iPPe copolymer (without added MDBS), but also with the expectation that RuO_4 serves as a preferential stain for MDBS under the staining conditions employed. (Under other conditions, RuO_4 can be used to stain the amorphous regions of polyolefins so that crystalline lamellae can be imaged with TEM.[25]) The few electron-opaque dispersions visible in Figure 6a are either residual catalyst particles or processing contaminants.

A network of fine, randomly oriented and

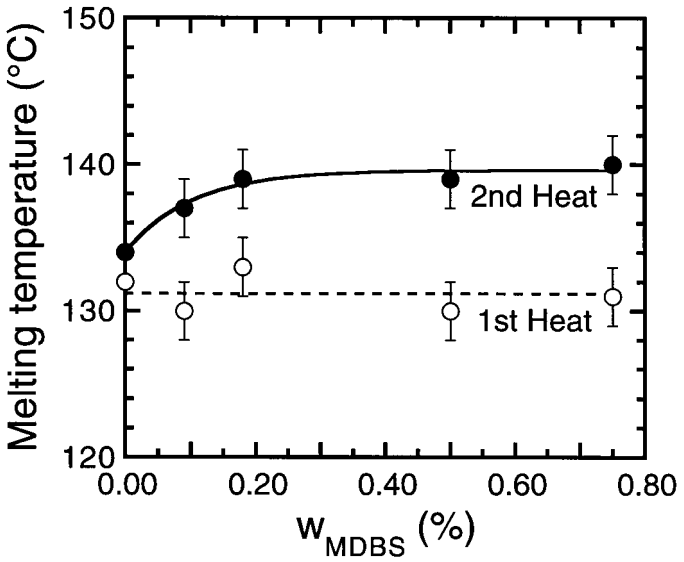

Figure 4. Melting temperatures as a function of w_{MDBS} from initial (○) and subsequent (●) DSC analyses performed at 10°C/min. The dashed line identifies the mean of the first heat data, while the solid line is provided as a guide for the eye. Vertical lines denote experimental error in the data.

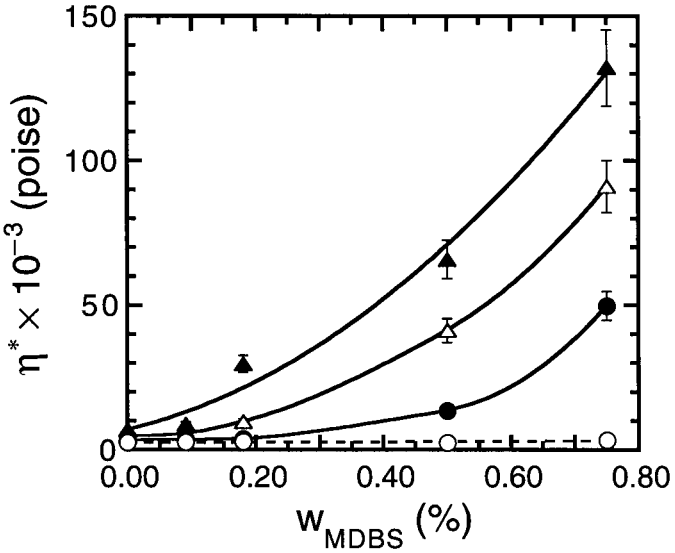

Figure 5. Dependence of η^* on w_{MDBS} for four different temperatures (in °C): 140 (▲), 160 (△), 180 (●), and 200 (○). Solid lines are guides for the eye and the dashed line is an average of the data evaluated at 200°C. Vertical lines correspond to ±10% experimental error in the data.

shaped nanofibrils measuring between 7 and 10 nm in diameter is evident (Fig. 6), even though the concentration of MDBS is only 0.09 wt % in this formulation. Note that the fibrils are clearly defined here due to the zero-loss imaging mode used to record the image on electron-sensitive plate film. In this mode, most of the inelastically scattered electrons produced during beam-specimen interaction are removed from image formation so that only unscattered or elastically scattered electrons are recorded.[26] While many of the fibrils in this micrograph appear to be singular, some isolated fibrillar clusters are also present. As w_{MDBS} is increased from 0.09 to 0.18, the formulation is found to consist of longer and more highly interconnected MDBS fibrils (Fig. 6c). Singular fibrils mainly comprising the network measure 7–13 nm across and are comparable in diameter (but not length) to those observed in the 0.09 wt % formulation (Fig. 6b). Thicker MDBS fibrils, or possibly fibrillar bundles, measuring up to about 80 nm in diameter are also visible (Fig. 6c). When the concentration of MDBS is increased to 0.50 wt % (Fig. 6d), the population density of fibrils, both thin (ca. 10–13 nm in diameter) and thick (ca. 100 nm in diameter), is seen to increase beyond that observed in the formulations with lower w_{MDBS} (Fig. 6b,c).

In Figure 6d a large fibrillar bundle appears to have been kinetically frozen as it began to either unravel into singular fibrils or elongate upon aggregation of singular fibrils. If such bundles become sufficiently numerous and large, they could alter the clarity of the material. We return to address this point below. It is also interesting to recognize that the MDBS fibrils in Figure 6d, unlike those in Figure 6b,c, are highly oriented along a single director. Such orientation is not characteristic of the entire specimen, but demonstrates that, due presumably to injection molding, the modified iPPe plaques may not be uniformly isotropic with respect to the MDBS nanofibrillar network. At the highest concentration of MDBS examined here (0.75 wt %), thin singular nanofibrils (8–13 nm in diameter) again appear to be prevalent, although some large-scale microstructural elements measuring up to ca. 200 nm across are also present in Figure 6e. In this micrograph, some of these large features are ellipsoidal in shape, while others appear to be more representative of hollow tubes observed at an angle in projection.

Figure 7a is a relatively low-magnification micrograph of one of the large-scale features present in the 0.75 wt % MDBS formulation. This microstructural element, similar to the one displayed in Figure 6d for the 0.50 wt % formulation, can be considered a highly organized fibrillar bundle. A higher magnification image of the bundle → fibril transition region is provided (Fig. 7b) and reveals that some of the singular MDBS fibrils exhibit a periodic structure along the fibrillar backbone. A through-focus series of electron micrographs, as well as adjustments to the objective

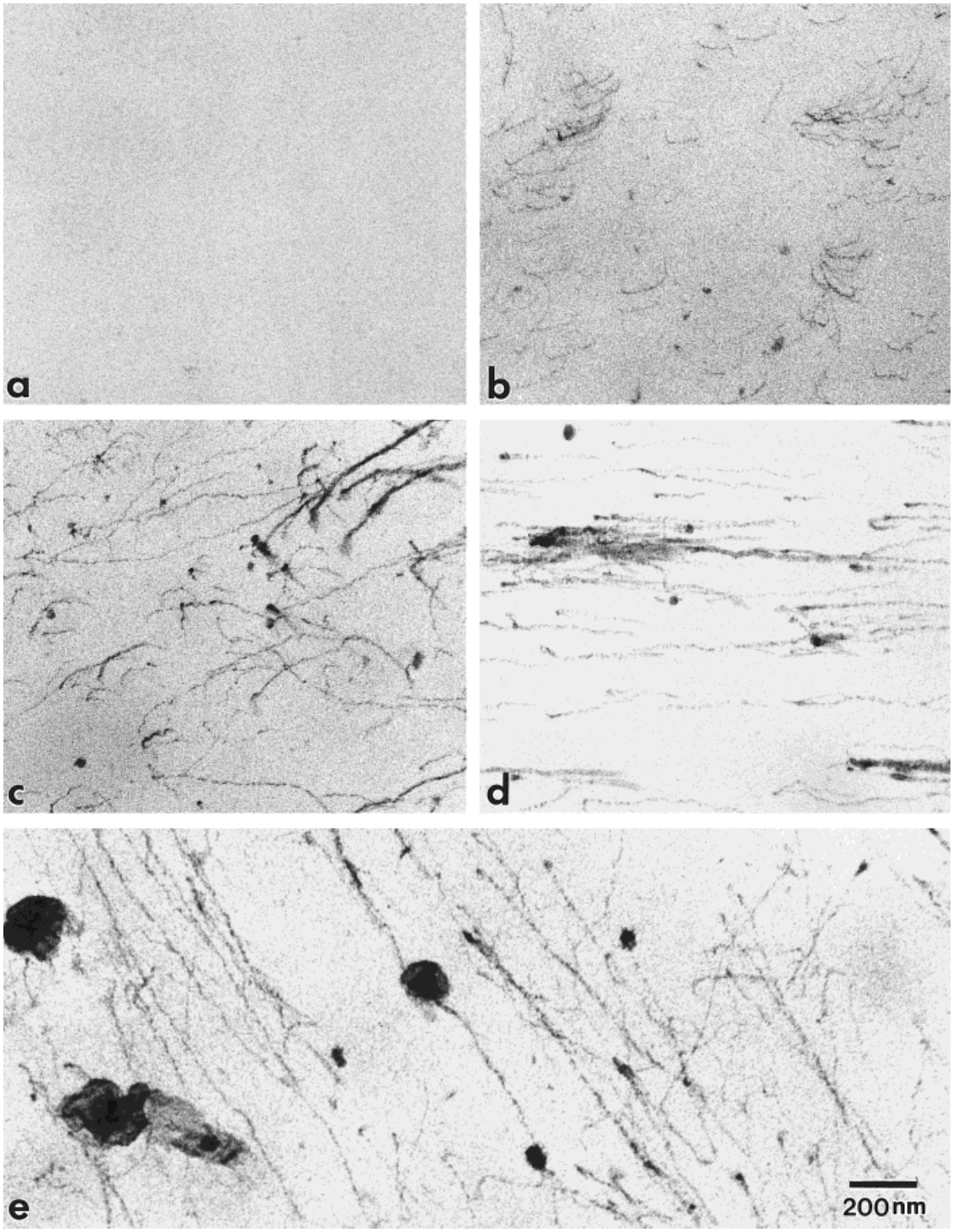

Figure 6. Transmission electron micrographs of the five iPPe/MDBS formulations examined here (in wt % MDBS): (a) 0.00, (b) 0.09, (c) 0.18, (d) 0.50, and (e) 0.75. Spheroidal dispersions such as those seen in (a) are artifactual. Nanofibrils composed of self-organized MDBS appear electron-opaque (dark) in (b)–(e) due to phenyl-specific RuO_4 staining.

astigmatism and energy filter, confirm that this structural characteristic is not artifactual in nature. It is also evident in the high-magnification micrograph shown in Figure 8 for a few isolated fibrillar strands in the 0.50 wt % MDBS formulation. Fourier analysis of Figure 7b and 8 (using

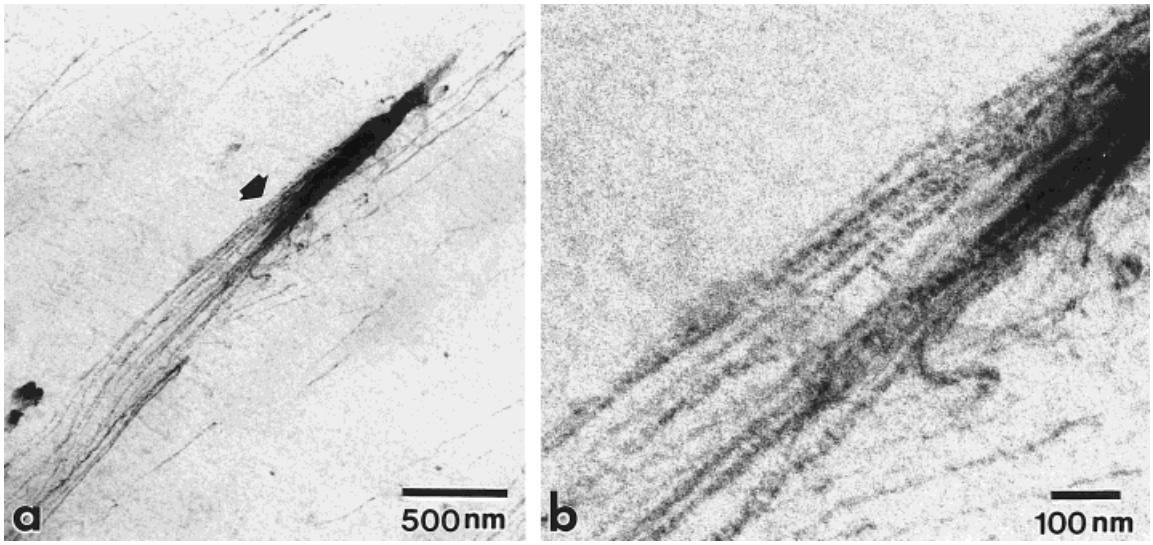

Figure 7. Electron micrographs of a highly organized fibril bundle in the 0.75 wt % MDBS formulation. The low-magnification image in (a) shows the length of the bundle and the presence of a transition region (arrowhead) at which the bundle unravels into singular fibrils or singular fibrils order into a bundle. A high-magnification image of the transition zone is provided in *b*.

the Digitalmicrograph® software package from Gatan Inc.) indicates that the period of the structure along the MDBS nanofibrils is about 15 ± 2 nm.

Such structure suggests that the nanofibrils observed in Figures 6–8 exhibit helical twist. It is important to note that such structure has been reported[5] (at a period of 11.0 nm) for fibrils of DBS derivatives deposited from solvent (e.g., 1,4-dioxane), subjected to negative staining (rather than the positive staining used here) and imaged with TEM. The presence of nanofibrillar twist is therefore at least qualitatively consistent with the structural model proposed by Yamasaki et al.[5] for self-organized DBS. In this model, the phenyl rings of aggregated DBS lie parallel to each other along the normal to the fibrillar axis. This arrangement facilitates hydrogen bonding be-

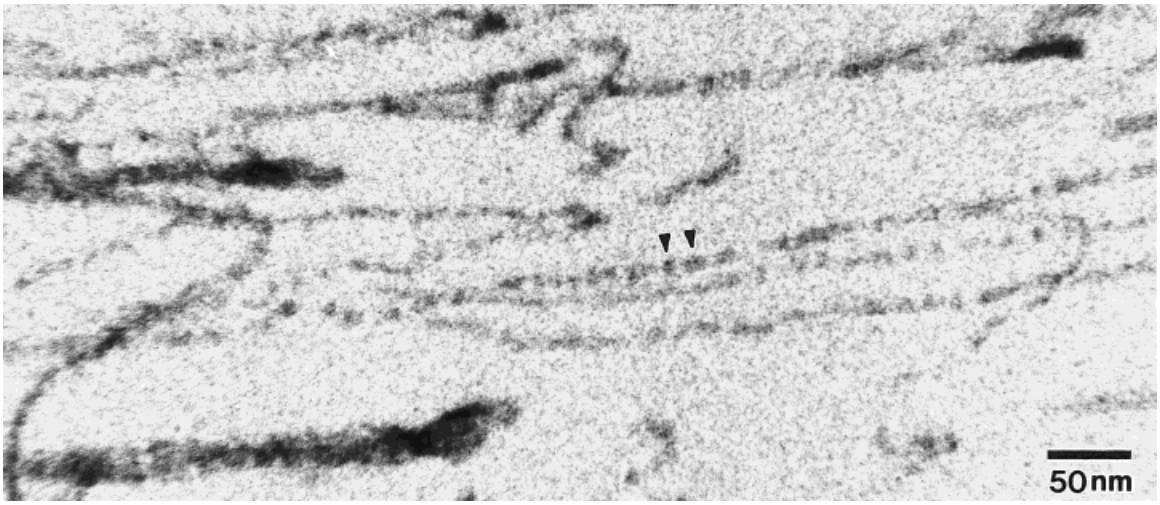

Figure 8. High-magnification image of MDBS nanofibrils that comprise the gel network in the 0.50 wt % MDBS formulation. Note the periodic structure (arrowheads) suggestive of helical twist along each of the nanofibrils (most easily seen when viewed at an oblique angle).

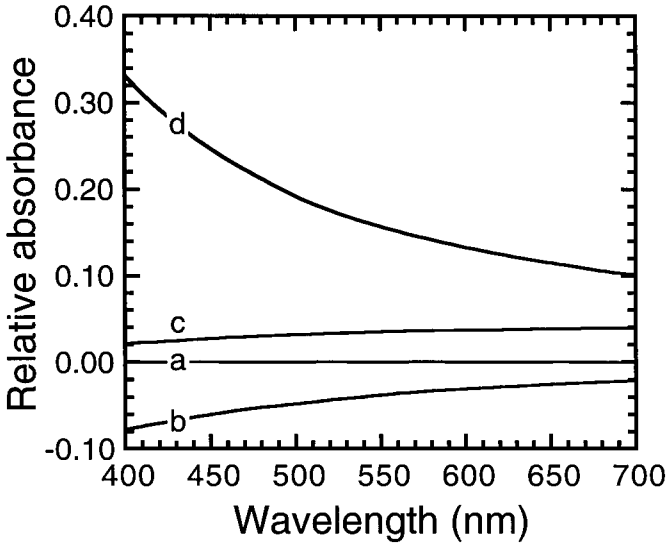

Figure 9. Absorbance relative to that of the unmodified iPPe copolymer presented as a function of wavelength for modified iPPe copolymers at four different MDBS concentrations (in wt %): (a) 0.09, (b) 0.18, (c) 0.50, and (d) 0.75.

tween the terminal hydroxyl group of one molecule and an acetal oxygen of another, verified through infrared analysis. While no attempt is made here to deduce the supramolecular structure of the MDBS nanofibrils seen in Figures 6–8, previous work addressing the organization of DBS molecules in low molar mass organic liquids indicates that the molecules are capable of ordering into a helical arrangement, which explains the periodic fibrillar structure seen in Figures 7b and 8.

Result of iPPe Crystal Nucleation

Due to the presence of an MDBS nanofibrillar network in the iPPe melt, heterogeneous nucleation of crystallizable iPPe macromolecules is greatly facilitated as the melt is cooled below T_c (see Fig. 2). We now describe how enhanced crystal nucleation affects some of the bulk properties of the iPPe copolymer. Figure 9 shows the absorbance of the MDBS-modified materials, relative to that of the unmodified iPPe copolymer, as a function of wavelength (λ). Since the optical properties of the formulation with only 0.09 wt % MDBS are not very different from those of the neat copolymer (curve a in Fig. 9), the relative absorbance is nearly zero over the entire range of λ examined. Upon addition of more MDBS (0.18 wt %, curve b), the relative absorbance curve decreases to below zero, indicating less absorbance or, conversely, more transmission of the incident beam through the specimen and, hence, greater clarity. Further increases of w_{MDBS} to 0.50 and 0.75 wt % (curves c and d, respectively) result in corresponding increases in relative absorbance beyond that of the neat copolymer. This means that these two formulations exhibit noticeably greater opacity than the neat iPPe copolymer (visually confirmed). Some of the data presented in Figure 9 are replotted as a function of w_{MDBS} for different λ in Figure 10 to more clearly illustrate the dependence of relative absorbance on MDBS concentration.

At long λ (700 nm), there is less variation in relative absorbance with w_{MDBS}, indicating that there are few composition-dependent structural characteristics at this length scale. At short λ (400 nm), however, the considerable increase in relative absorbance of the 0.75 wt % formulation may be due to large-scale microstructural aggregates (see Figs. 6 and 7), which, if sufficiently numerous, could cause a substantial reduction in beam transmission and a corresponding increase in measured absorbance due to scattering. Scattering from such large structures would certainly explain why the 0.75 wt % formulation appears the most opaque of the series. Thus, the efficient use of DBS as a clarifying agent in polyolefins must balance two considerations. Nucleation of the polyolefin crystals results in enhanced clarification due to less scattering from spherulites of reduced size. This apparent reduction in spherulite size is consistent with the findings of Sterzynski et al.,[17] who have reported a 50× reduction in spherulite size (from 50 μm down to 1 μm in dia-

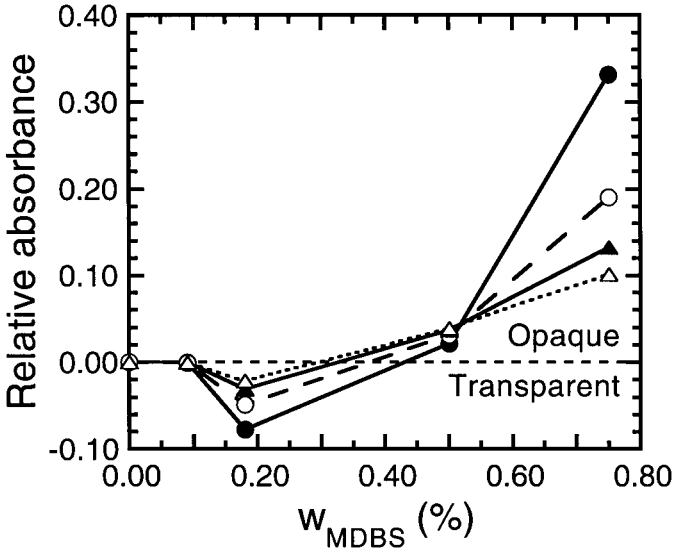

Figure 10. Absorbance relative to that of the neat iPPe copolymer presented in terms of w_{MDBS} for four different wavelengths (in nm): 400 (●), 500 (○), 600 (▲), and 700 (△). Below the horizontal dashed line at 0.00, the formulation exhibits greater clarity than the neat copolymer; above this line, greater opacity is observed. The remaining lines connect the data points.

meter) upon the addition of MDBS to a random iPPe copolymer of comparable composition to the one employed here. Recall, however (Figs. 3 and 4), that the nucleation efficacy of DBS appears to reach a saturation level at relatively low w_{MDBS}. Beyond the onset of this saturation level, additional DBS appears to have little, if any, effect on the polyolefin crystals. Instead, as seen in Figure 6, an increase in w_{MDBS} promotes coarsening of the DBS fibrillar network, eventually resulting in the formation of structural elements sufficiently large to scatter light and reduce clarity.

Another consequence of nucleated iPPe crystals in these MDBS formulations is mechanical property enhancement. We provide some of the results obtained from the iPPe/MDBS formulations when subjected to uniaxial tensile deformation at ambient temperature. The results presented in the following figures reflect at least six specimens tested at each MDBS concentration. Shown in Figure 11 is the yield strength of these formulations as a function of w_{MDBS} for two different crosshead speeds. Consistently higher yield strengths are expected, and observed, from measurements conducted at faster crosshead speeds, since the polymer chains have less opportunity to relax under the applied load than at slower crosshead speeds. As seen in Figure 11, an increase in w_{MDBS} is accompanied by an initial increase, followed by a constant-level plateau, in yield strength at both crosshead speeds. Note that the faster crosshead speed produces a slightly greater difference between the yield strength of the unmodified copolymer and that of the high-w_{MDBS} plateau (4.3 MPa at 2.5 mm/min vs. 5.2 MPa at 25 mm/min). These plateau values correspond to MDBS-induced increases in yield strength of about 20% (relative to the non-

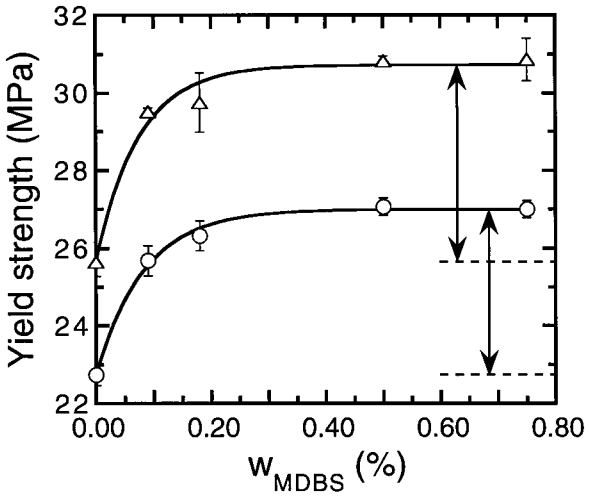

Figure 11. Yield strengths from uniaxial tensile measurements as a function of w_{MDBS} for two crosshead speeds (mm/min): 2.5 (○) and 25 (△). Dashed lines denote the yield strength of the neat iPPe copolymer, and the arrows show the maximum difference in yield strength at high w_{MDBS}. Solid lines are guides for the eye and error bars denote 1 SD in the data.

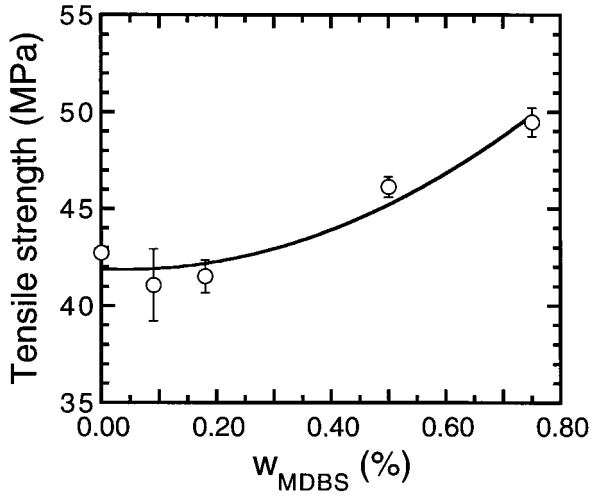

Figure 12. Variation in the tensile strength of the MDBS-modified iPPe formulations with w_{MDBS} upon uniaxial tensile deformation at a crosshead speed of 2.5 mm/min. The solid line is provided as a guide for the eye and error bars denote 1 SD in the data.

nucleated iPPe copolymer), which is slightly higher than the 14% reported elsewhere.[17]

The trends evident in Figure 11 are surprisingly comparable to those found earlier for the crystallization and melting temperatures of the MDBS-nucleated iPPe formulations (see Figs. 3 and 4), and support the observation made earlier that the effectiveness of MDBS to induce iPPe crystal nucleation saturates at relatively low w_{MDBS}. Beyond the onset of this level, additional MDBS appears to be of no further benefit to the properties derived from the iPPe crystals. Whereas the yield strength is principally a probe of the iPPe matrix (including the crystal, intercrystalline, and amorphous regions), the tensile strength depends on contributions from both the iPPe matrix and the three-dimensional MDBS nanofibrillar network. The variation of tensile strength with MDBS concentration is displayed in Figure 12 and reveals that, at low w_{MDBS}, there is virtually no change (within experimental error) in tensile strength due to existence of the MDBS network. At higher MDBS concentrations, however, the tensile strength is found to increase by as much as about 16% at 0.75 wt % MDBS.

Another mechanical property that appears to be affected by the MDBS network is the elongation at break, which is defined as the strain at which fracture occurs upon uniaxial tensile deformation. As seen in Figure 13, the elongation decreases initially with increasing w_{MDBS}, which is unexpected due to the reduction in spherulite size (and the increase in spherulite surface area) accompanying MDBS-induced nucleation of the iPPe copolymer. As w_{MDBS} is increased further, however, the elongation at break likewise increases (by more than 12% for the 0.75 wt % formulation, relative to the unmodified iPPe copolymer). While the precise molecular mechanism responsible for the observed increase in elongation with increasing w_{MDBS} remains unclear at this time, it is anticipated that the smaller (nucleated) iPPe spherulites, in conjunction with the three-dimensional MDBS nanofibrillar network, are responsible for reinforcing the iPPe chains in the modified copolymers, thereby requiring a greater strain to induce specimen failure. It is of interest to note here that increases in both tensile strength and elongation at break are also generally indicative of an increase in fracture toughness (not measured here).

CONCLUDING REMARKS

Addition of small quantities (<1 wt %) of 1,3:2,4-di-*p*-methylbenzylidene sorbitol (MDBS) to an isotactic polypropylene copolymer with 3 wt % ethylene (iPPe) results in the formation of a three-dimensional network of MDBS nanofibrils that measure on the order of 10 nm in diameter. These nanofibrils are comparable in thickness to those observed[7–9,12] in DBS-modified polydimethylsiloxane homopolymers and graft copolymers. At low concentrations of MDBS, the nanofibrils

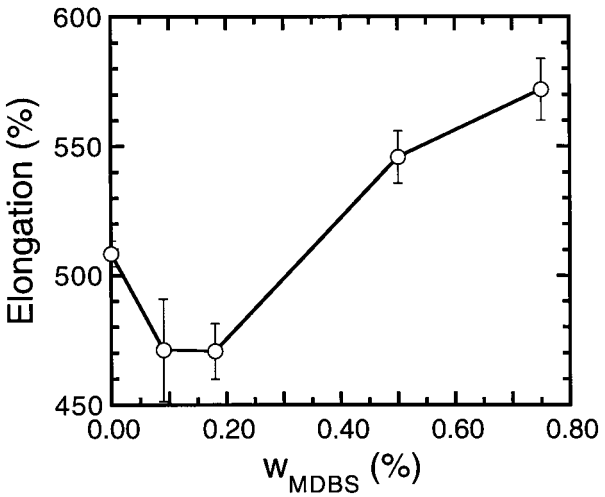

Figure 13. Elongation at break of the MDBS/iPPe formulations as a function of w_{MDBS} upon uniaxial tensile deformation at a crosshead speed of 2.5 mm/min. The solid line connects the data points, and error bars denote 1 SD in the data.

serve as nucleation sites to induce heterogeneous nucleation of iPPe spherulites, resulting in clarified formulations with enhanced yield strength and marginally higher melting temperatures. As the concentration of MDBS is increased, no additional benefit to iPPe crystal nucleation is achieved, suggesting that nucleation efficacy saturates at relatively low MDBS concentrations. Under these conditions, the nanofibrils coarsen, and the population of fibrillar bundles, as well as cylindrical/tubular microstructures measuring up to ca. 200 nm in diameter, is found to increase. While these large-scale microstructures reduce optical clarity, they may likewise be responsible for improving some of the ultimate mechanical properties (e.g., tensile strength and elongation at break) at high MDBS concentrations. These results indicate that MDBS added to a polyolefin may serve as either a nucleating or clarifying agent at low concentrations, or a reinforcing agent at high concentrations.

We are grateful to Drs. C. M. Balik and C. K. Chiklis for valuable discussions, and to Dr. B. Hsiao for performing the wide-angle x-ray diffraction analysis.

REFERENCES AND NOTES

1. E.-L. Roehl and H.-B. Tan, *U.S. Patent* 4,154,816, May 15, 1979.
2. S. Yamasaki and H. Tsutsumi, *Bull. Chem. Soc. Jpn.,* **67,** 906 (1994).
3. S. Yamasaki and H. Tsutsumi, *Bull. Chem. Soc. Jpn.,* **67,** 2053 (1994).
4. S. Yamasaki and H. Tsutsumi, *Bull. Chem. Soc. Jpn.,* **68,** 123 (1995).
5. S. Yamasaki, Y. Ohashi, H. Tsutsumi, and K. Tsujii, *Bull. Chem. Soc. Jpn.,* **68,** 146 (1994).
6. A. Thierry, B. Fillon, C. Straupé, B. Lotz, and J. C. Wittmann, *Progr. Colloid Polym. Sci.,* **87,** 28 (1992).
7. J. R. Ilzhoefer and R. J. Spontak, *Langmuir,* **11,** 3288 (1995).
8. J. M. Smith and D. E. Katsoulis, *J. Mater. Chem.,* **5,** 1899 (1995).
9. T. A. Shepard, *M.M.S.E. Project Report,* North Carolina State University (1995).
10. C. M. Nuñez, J. K. Whitfield, D. J. Mercurio, J. R. Ilzhoefer, R. J. Spontak, and S. A. Khan, *Macromol. Symp.,* **106,** 275 (1996).
11. D. J. Mercurio, S. A. Khan, and R. J. Spontak (manuscript in preparation).
12. J. R. Ilzhoefer, B. C. Broom, S. M. Nepa, E. A. Vogler, S. A. Khan, and R. J. Spontak, *J. Phys. Chem.,* **99,** 12069 (1995).
13. D. Mitra and A. Misra, *Polymer,* **29,** 1990 (1988).
14. T. Kobayashi, H. Hasegawa, and T. Hashimoto, *Hihon Reoroji Gakkaishi,* **17,** 155 (1989).
15. T. Kobayashi, M. Takahashi, and T. Hashimoto, *Hihon Reoroji Gakkaishi,* **18,** 155 (1990).
16. I. Dolgopolsky, A. Silberman, and S. Kenig, *Polym. Adv. Technol.,* **6,** 653 (1995).
17. T. Sterzynski, M. Lambla, H. Crozier, and M. Thomas, *Adv. Polym. Technol.,* **13,** 25 (1994).
18. T. L. Smith, D. Masilamani, L. K. Bui, Y. P. Khanna, R. G. Bray, W. B. Hammond, S. Curran, J. J. Belles, and S. Bindercastelli, *Macromolecules,* **27,** 3147 (1994).
19. C. Y. Kim, Y. C. Kim, and S. C. Kim, *Polym. Eng. Sci.,* **33,** 1445 (1993).
20. M. Fujiyama and T. Wakino, *J. Appl. Polym. Sci.,* **42,** 2739 (1991).
21. M. Fujiyama and T. Wakino, *J. Appl. Polym. Sci.,* **42,** 2749 (1991).
22. Y. C. Kim, C. Y. Kim, and S. C. Kim, *Polym. Eng. Sci.,* **31,** 1009 (1991).
23. D. Mitra and A. Misra, *J. Appl. Polym. Sci.,* **36,** 387 (1988).
24. B. Hsiao, private communication (1995).
25. J. S. Trent, J. I. Scheinbeim, and P. R. Couchman, *Macromolecules,* **16,** 589 (1983).
26. L. Reimer, in *Energy-Filtering Transmission Electron Microscopy,* L. Reimer, ed., Springer-Verlag, Berlin, 1995, Chap. 7, pp. 347–363.